

# A fully autonomous docking strategy for Intervention AUVs

L. Brignone, M. Perrier, and C. Viala

**Abstract**—The development of effective control architectures for Intervention AUVs (I-AUV) is a very challenging task due to the inherent complexities of the environment and the necessity of the vehicle to come into contact with underwater structures without closed-loop supervision. Despite this, both the scientific and industrial communities are keen supporters of the development of I-AUV technology owing to the relevant cost saving opportunities they are potentially able to offer in a number of applications.

In this article we describe a comprehensive control architecture designed to dock an I-AUV on a receiving structure, using sonar and video image processing alongside navigation data from conventional sensors. The approach is based on custom developed sonar and video processing algorithms and the results are validated in real-time conditions by means of Ifremer's experimental underwater vehicle VORTEX.

## I. INTRODUCTION

The continuous improvements in performance of energy storage technology, the precision of navigation instruments and the reliability of acoustic communication devices, has enabled Autonomous Underwater Vehicles (AUV) to spawn from R&D and university into direct employment in an ever increasing number of industrial, scientific and military applications. Although these are in general restricted to a variety of survey type tasks, non-hovering AUVs have proven to be more successful than towed or remotely operated solutions, both in terms of cost effectiveness (subsea survey, pipeline/cable inspection, environmental monitoring) and of feasibility (sub-ice survey and ultra-deep water).

It is a widely accepted idea however that more interesting technological opportunities lie in the domain of underwater intervention, where the use of *hover capable* AUVs could contribute to increased efficiency and relevant cost reductions. The first hand experience of the SIRENE [1], SWIMMER [2] and ALIVE [3] European projects, in which IFREMER

contributed to develop core modules such as control, navigation and communication, leads to the identification of two major limitations of Intervention AUVs (I-AUV). First of all, compared to a general purpose survey AUV, an I-AUV offers a less re-configurable platform, featuring a tailor made architecture developed for a specific task. Secondly, the restrictions in available energy mean that only light intervention tasks can be performed by a fully autonomous system.

Despite these limitations, recent times have witnessed an increased interest in the development of I-AUVs as they are set to benefit from the aforementioned technological improvements. This is for instance the case of the SWIMMER autonomous vector/lander designed to transport a small work class ROV and connect it to power and control lines by docking to a purposed built station on the seabed. This hybrid solution has recently reached a new development stage, fuelled by interest from major oil companies.

The subsequent development of the ALIVE vehicle has represented a further and fundamental technological step forward. The principle demonstrated in the course of the three year European project, is simple and yet embodies all of the complexities of autonomous underwater intervention: an AUV designed to dock automatically on a wellhead structure and to operate a series of controls by means of a manipulator arm.

A further interesting example is the implementation of the SEA-BEE concept [4], showing the possibility to combine small-range survey capabilities and autonomous seabed core sampling for scientific and environmental analysis. The principle was demonstrated through the use of the ALIVE platform, fitted with specific equipment and modifications.

The SUBTECH project we are currently developing provides a new opportunity to further improve the methodologies and ideas implemented in the aforementioned approaches. The project aims at developing a comprehensive technique to perform a quadri-dimensional analysis (e.g. position and time) of the seismic activity in an area of interest. The approach is based on the use of battery-powered ocean bottom seismic sensors (OBS) which are designed to be carried, placed and retrieved automatically by an AUV. IFREMER, Cybernetix and CGG are development partners within the project, working respectively on the task of autonomous docking, intervention by means of a robotic arm and OBS development.

In this paper we present the principles of a comprehensive

Manuscript received February 21, 2007. This work was supported in part by the French oil and gas industry committee CEP&M and the other partners of the SUBTECH project (IFREMER, CYBERNETIX, CGG).

L. Brignone is a development engineer in the Underwater Systems Department at IFREMER (France) (phone: 0033 (0)494304935 e-mail: lorenzo.brignone@ifremer.fr).

M. Perrier, is the director of the *Positioning, Acoustics, Vision and Robotics* division of IFREMER's Underwater Dept. (e-mail: michel.perrrier@ifremer.fr).

C. Viala is CTO of the French SME Semantic TS specialised in sonar signal processing (e-mail: viala@semantic-ts.fr).

docking technique that involves the use of a passive acoustic marker and related sonar signal processing for identifying the OBS seabed installation from distances up to 50m, and a vision based final approach controller. The two modules enable the vehicle controller to identify, navigate to and dock onto the OBS seabed installation structure fully autonomously, i.e. without recurring to operator step-by-step validation as featured in earlier attempts.

## II. DOCKING AND THE MISSION SCENARIO

The ability to dock to a fixed seabed structure is an important prerogative of I-AUVs, which exploit their hover capabilities and use locally sensed information to perform fine motion control prior to contact. Docking is also often a necessary condition to support the intervention task as it enables to:

- 1) reduce the degrees of freedom (DOF) of the vehicle;
- 2) reduce the risk of collisions associated with DP hovering;
- 3) attain a known/sought geometric configuration with the structure to intervene on;
- 4) reduce vision perturbation by allowing total/partial thruster shut off during intervention;
- 5) mate compliant connections in a known geometric environment;
- 6) compensate for changes in weight balance on the AUV that may occur during intervention.

Examples of applications that require docking include, but are not restricted to, wellhead inspection/intervention, connection to power/data lines, equipment placing and removal. Using similar techniques, an I-AUV may also be designed to dock onto vertical rigid or semi-rigid structures, such as pillars, chains or risers to perform local inspection or even intervention tasks. Finally, safe landing procedures are to be employed in case the I-AUV is due to perform an intervention directly on the seabed as opposed to a manmade structure.

In order to regulate the contact with the structure/object of interest, the vehicle's motion controller needs to be fed with high accuracy kinematic data, describing relative pose and positioning between the mobile and the fixed bodies. The actual docking is then performed as a pre-programmed task, often exploiting mechanical compliance in the mating ends.

Sensed information includes sonar and image data, which is necessary both to detect and recognise the sought structure and to overcome the shortcomings of traditional navigation data. These include drift in dead reckoning estimation, the need of acoustic fixes to improve accuracy, and the inoperability of certain sensors at close range from the seabed (as is the case with Doppler velocity logs - DVL).

As mentioned above our aim is to develop a fully autonomous docking methodology, without the presence of an operator in the loop to validate the different phases of the mission. Starting our design analysis from the geometry of the OBS (see Fig. 1) and the kinematics of its placement/retrieval from the seabed installation, we have

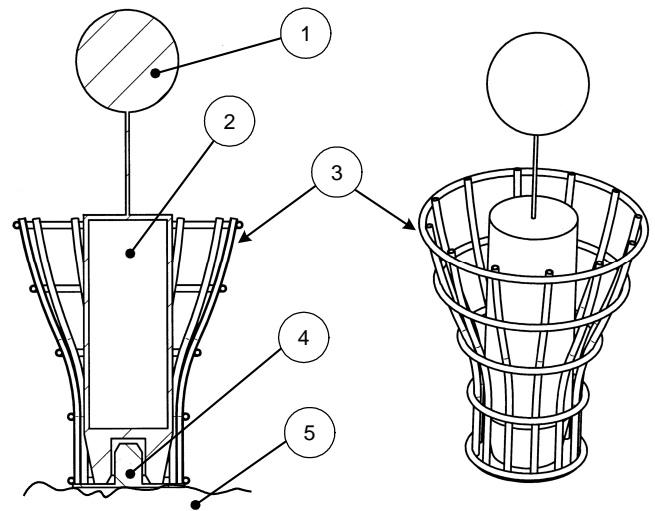


Fig. 1. OBS section (left) and prospective view (right) featuring: 1) float, 2) cylindrical pressure housing (L=1.2m,  $\Phi=0.3$ m) 3) compliant receptacle for vertical insertion/extraction 4) seismic sensor seabed induction connector 5) seabed

conceived a docking strategy that includes:

- 1) the use of passive acoustic and video markers on the docking structure to improve efficiency of detection and pose/position estimation;
- 2) axisymmetrical docking strategy, allowing the vehicle to approach and connect to the structure from any direction in the plane;
- 3) simplified *thrust-on* mechanical docking;
- 4) robustness towards docking failure.

In our case, a typical mission scenario features four subsequent stages, during which the AUV detects and identify the OBS structure, navigates towards it, docks onto it and finally performs a pre-programmed manipulation task (OBS swap).

### A. Detection and identification

As a result of the joint effect of navigation inaccuracy and the uncertainty of the precise location of the docking structure, an initial phase of detection and identification of the target is necessary. This is also necessary when the I-AUV has completed the intervention on one OBS and needs to navigate to the presumed location of the next. To address to these needs, we have introduced a sonar processing algorithm to identify the specific acoustic signature of a passive marker placed in the OBS structure. The geometrical solution we have developed for the marker allows detection to be axisymmetrical. The implementation of the filtering algorithm is detailed in the next section of this article, showing the ability to detect the marker in terms of range  $\hat{\rho}$  and bearing  $\hat{\vartheta}$  at distances exceeding 40m from the vehicle. The use of a mechanically scanned sonar head (in our case a *Tritech SuperSeaking<sup>®</sup> DST*) suits well the proposed method.

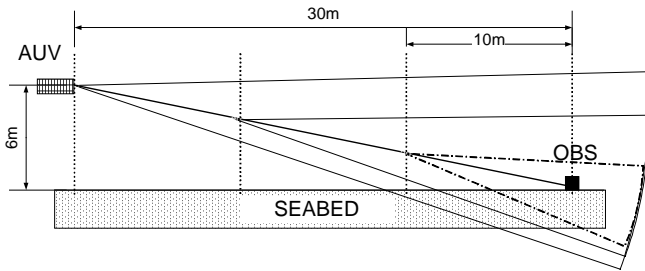


Fig. 2. Vehicle glidepath towards OBS considering  $20^\circ$  sonar vertical beamwidth; the altitude setpoint is updated continuously to match path as function of target distance.

### B. Navigation towards the OBS

Following positive identification, the vehicle navigates towards the target, modifying the altitude and longitudinal speed setpoint as it approaches. During this phase the vehicle's sonar head is constantly panned as the acoustic response is treated feeding the control algorithm with updated bearing and range to target. Considerations on the vertical beamwidth of the sonar and its mounting angle must be made in order to adapt the AUV's altitude to maintain the target well within the beam (see Fig. 2) up to visual range (2m to 3m). An extended Kalman filter is used to merge the estimated bearing/range information with further navigation data (vehicle heading and velocity); this also serves to reject outliers and manage temporary detection losses. The Kalman filter implemented is essentially a two-dimensional filter, providing corrected target planar coordinates by feeding forward the estimated position and velocity of the vehicle and correcting them respectively with OBS sonar fix and DVL measurements as they become available.

### C. Fine alignment and docking

Once the vehicle is finally at close range from the OBS (2m to 3m), the control is automatically switched over to the vision control system that processes the image from the onboard camera and computes an appropriate thrust vector to bring the vehicle to the intended docking configuration. The transition from sonar referenced to vision referenced is performed *automatically* by evaluating an *index of confidence* calculated as a byproduct of the image processing. This is described in more detail in the next section. Being the altitude of the docking ring a known geometrical parameter, the vehicle's altitude is controlled in the final stages of the vision based approach. Docking is performed by thrusting to maintain contact between two passive grabbers at the front end of the vehicle (fitted with dampers) and a docking ring located in the topmost section of the OBS structure. The vertical span of the grabbers compensate for vertical misalignment and heave oscillations, acting as a guide for the vehicle as it moves forward (Fig. 3 (9)). The maneuver is axisymmetrical, as the vehicle can approach and dock from any direction on the plane (see Fig. 3 which shows VORTEX in the role of the I-AUV).

### D. Manipulation task

Having attained a fixed geometrical configuration between

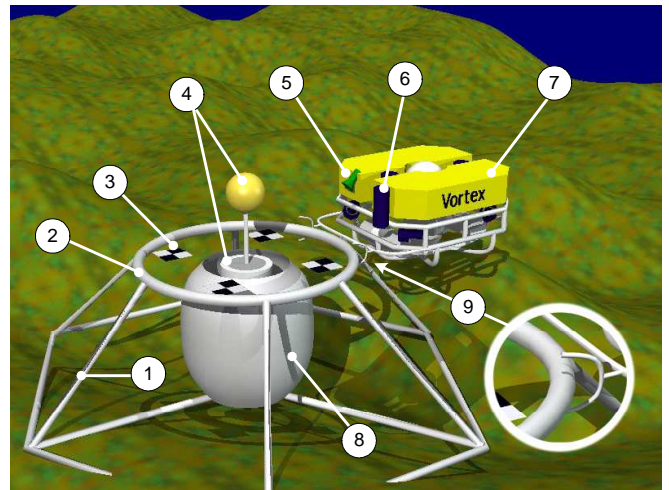


Fig. 3 – General view at docking featuring IFREMER's Vortex as test mock up 1) Docking structure 2) Docking ring 3) optical marker 4) OBS and float 5) camera 6) sonar 7) I-AUV 8) sonar marker 9) passive grabber closeup

vehicle and OBS, the vehicle's manipulator arm is deployed to remove the OBS (Fig. 1) from the seabed structure and replace it with a new one. This part of the project is currently being developed by Cybernetix and will be detailed in a later article.

## III. SONAR SIGNAL PROCESSING

Our technique for detecting seabed stations is based on the use of a passive marker to produce a specific acoustic response while reflecting incoming sonar pulses. Moreover we decided to avoid to represent the reflected signal in cartesian space and process it as an image, but rather develop an algebraic procedure to treat the acoustic response numerically. This has the double advantage to allow faster detection (range and bearing) and to be well suited to a mechanically scanned sonar head, as each angular step response is treated without waiting for a full sector to be completely scanned.

### A. Geometrical configuration of the passive marker

The development of the geometrical characteristics of the passive markers is the key factor in the methodology and is based on three main properties:

- 1) to be highly reflective;
- 2) to provide a distinct multiple response to enable identification in noisy and unknown environment;
- 3) to suit the approach technique envisaged (see Fig. 2).

The design is therefore based on an empty and axisymmetrical aluminium shell that responds with multiple echoes as the acoustic pulse is reflected first on its external face and several times on the opposite one afterwards.

Three shapes were at first considered, the barrel being chosen over the cylinder and a double inverted cone after initial tests using a Simrad single beam echosounder (200kHz to 1 MHz). The barrel has in fact proven to ensure an acoustic response featuring two distinct peaks, spaced of a length consistent with the geometry of the marker itself (see Fig. 4).

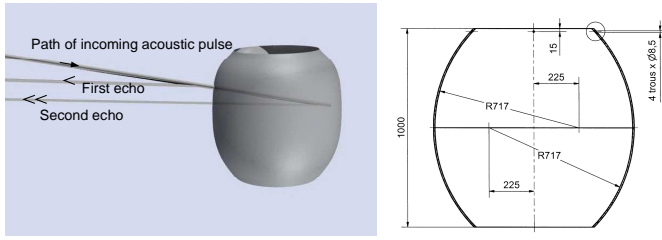


Fig. 4 – Principle of passive marker multiple echoes (left) – overall marker geometry featuring equal curvature radii (right).

Moreover the measured spacing is constant with respect to the tested ranges (5m to 45m) and angles of incidence (6° to 45°). Typical values measured for the spacing  $d^*$  between the peaks range between 1.2m and 1.3m in the case of our marker prototype built according to the dimensions in Fig. 4 (right). This is in turn the distinctive acoustic trace that the processing algorithm uses to identify the marker and detect it over a noisy environment.

### B. Sonar processing algorithm

The processing technique is based on the numerical normalisation of the incoming raw acoustic signal  $R$  and it involves sliding over  $R$  two averaging operators  $\mu_A$  and  $\mu_B$  of identical and predetermined width (Fig. 5). Since  $R$  is referenced to the distance traveled by the acoustic echo, the spacing between the two averaging windows can be set to be equal to the expected distance between the two peaks  $d^*$ . This will bring  $R_{NORM}$  to reach maximum intensity when two subsequent peaks spaced by  $d^*$  are encountered in the source signal  $R$ .

More precisely, the computation of the normalised signal  $R_{NORM}$  follows these equations:

$$R_{NORM} = \begin{cases} \frac{R - \mu_A}{\sigma_A} & \text{if } \mu_A = \min(\mu_A, \mu_B) \\ \frac{R - \mu_B}{\sigma_B} & \text{if } \mu_B = \min(\mu_A, \mu_B) \end{cases} \quad (1)$$

where  $\sigma_A$  and  $\sigma_B$  indicate the standard deviation values of  $R$  in the averaging window.

The resulting normalised curve is subsequently thresholded using a discriminant value defined experimentally, to decide whether the input signal  $R$  contains the marker's signature. The estimated range of the marker from the vehicle's sonar is then identified as:

$$\hat{\rho} : R_{NORM}(\hat{\rho}) = \max(R_{NORM}) \quad (2)$$

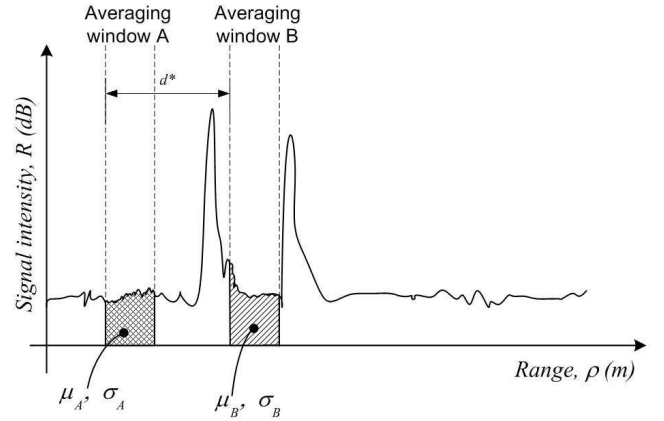


Fig. 5 – Elements used in the computation of  $R_{NORM}$

### C. Marker detector software implementation

The signal processing algorithm has been successfully adapted to the sonar chosen for real-time implementation, a *SuperSeaking DST* mechanically scanned dual frequency head produced by *Tritech International*.

The sonar is connected via RS232 link to the vehicle's onboard PC where the marker detector software (MDS) is running. The lack of a dedicated process unit simplifies greatly the task of onboard integration, and it is one of the reasons behind the choice of this type of system. We have custom developed a software interface enabling the MDS to program the parameters of interest in the sonar head such as: range, linear resolution, angular step size, frequency (low 325 kHz, high 675 kHz), bearing and dimension of the sector to be scanned. The software interface allows also to retrieve the encoded acoustic response curve  $R$ , for which we have chosen 8 bit resolution and 800 samples. As an example, this means that selecting a maximum range of 40m, the theoretical range resolution of the returned echo is:

$$\frac{40[m]}{800} = 0.05m \quad (3)$$

ensuring adequate resolution, as the characteristic peak spacing  $d^*$  measures about 25 times that value.

During operation the MDS works in closed loop with the sonar head, retrieving and processing an 8 bit encoded acoustic response at a time. If the correspondent  $R_{NORM}$  passes the set threshold, the range of the identified object is found according to (2).

This information (positive detection and range) is then completed by the bearing  $\hat{\vartheta}$  of the identified object, which is computed and related to magnetic North using the measured vehicle heading from the onboard fluxgate compass, and the angular position of the sonar head corresponding to the input signal  $R$ .

The MDS finally outputs to the navigation Kalman filter the estimated target range and bearing  $\rho^*, \vartheta^*$ , whose values are averaged over individual  $\hat{\rho}, \hat{\vartheta}$  pairs corresponding to adjacent

$R$  curves (in terms of angular position) whose  $R_{NORM}$  has passed the detection threshold.

#### D. docking structure architecture

The overall dimensions of the passive sonar marker allow simple integration in the docking structure, whose design is finalised (see Fig. 3) and includes:

- 1) a tubular protecting structure
- 2) the support for the OBS
- 3) the passive sonar marker
- 4) the docking ring
- 5) optical markers

When the OBS is inserted in its receptacle, it partially fills the water volume contained in the passive marker. This has however not shown to affect the detection of the marker, as the reflected acoustic signal still maintains the two distinctive peaks. The presence of the OBS generally lowers the intensity of the second peak and causes further echoes, which are however located further away in the acoustic response. These additional echoes feature a much lower intensity, which is consistent with their delay compared to the main two peaks, as the acoustic pulse is reflected (and attenuated) several times before exiting the barrel.

#### IV. VIDEO PROCESSING ALGORITHM FOR FINAL ALIGNMENT AND DOCKING

For final alignment and docking we have opted for an image-based control technique, that aims at adapting the position of the vehicle in order for a set of visual features  $\mathbf{s}$  to reach a desired configuration  $\mathbf{s}^*$  in the scene observed by the onboard camera. Such visual features usually correspond to a set of points chosen *a priori* on the target. Unlike model based position control, the pose of the camera is not explicitly estimated, but displacements are rather computed in 2D image space in order to reach the desired configuration. The output of the algorithm is a set of computed velocities in camera reference frame, which are then converted into thruster commands in vehicle frame through an appropriate transformation matrix and a set of proportional gains. Therefore the setpoint for the control algorithm is expressed as a desired configuration  $\mathbf{s}^*$ , corresponding to a set of  $x, y$  coordinates in image space of the visual features observed by the camera at docking position. The input of the controller is on the other hand the current image in which to identify the visual features  $\mathbf{s}$ .

The control algorithm is consequently based on three main operations: 1) the *identification in the image space* of the visual features sought for, 2) the *computation of camera velocities* necessary to attain target configuration  $\mathbf{s}^*$ , 3) the *conversion in vehicle frame* in terms of thruster commands. A brief description of the first two and more important stages follows.

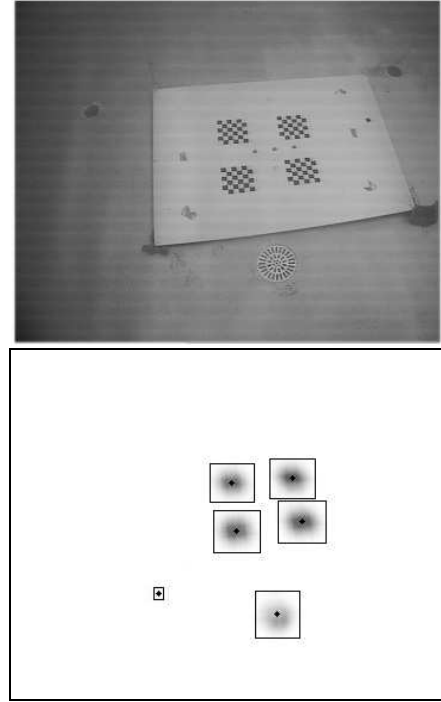


Fig. 6 – Image processing experiment in IFREMER's test pool. Original image (top) and processed image before binarisation (bottom) where marker positions are identified as well as some false detection (i.e. the pool's drain).

#### A. Identification of visual features

In order to increase the robustness of the features detection algorithm towards the disturbances typically affecting underwater scenes (absorption, low visibility, bio fouling) we have opted for four checkered patterns positioned within the docking ring forming a square pattern (see Fig. 3 (3)).

The central points of the markers are identified in the source image by successive filtering, based on a sequence of Harris corner detector [5], adaptive binarisation and morphological union operator. As a result, high contrast areas of the original image are transformed into blobs in a binary image (see Fig. 6). False detections are rejected with geometrical considerations –size and square pattern formed by the centres of the detected blobs- or by running cross correlation on the extracted areas to find the four matching ones. Both techniques have proven to work well during our test tank trials, the second technique being computationally heavier.

#### B. Computation of camera velocities

Computation is performed using the 2½D technique described in [6].

In the camera pinhole model, the relationship between a point  $P(X, Y, Z)$  in 3D space and its correspondent  $\mathbf{s}(x, y)$  on the 2D image space is expressed perspective projection equations which considering  $l$  as the focal length, indicate:

$$x = \frac{l}{Z} X \quad , \quad y = \frac{l}{Z} Y \quad (4)$$

On the other hand the relationship between the time variation of a feature  $\mathbf{s}$  in image space and the velocity of the

camera  $\mathbf{v} = [v^x \ v^y]^T$  is expressed by the image Jacobian matrix (or interaction matrix)  $\mathbf{L}$  which relates to the differentiation of (1):

$$\dot{\mathbf{s}} = \mathbf{L}(\mathbf{s}, Z)\mathbf{v} \quad (5)$$

A typical form of  $\mathbf{L}$  for a given feature  $\mathbf{s}$  whose depth in space is  $Z$  is:

$$\begin{pmatrix} -1/Z & 0 & x/Z & xy & -(1+x^2) & y \\ 0 & -1/Z & y/Z & 1+y^2 & -xy & -x \end{pmatrix} \quad (6)$$

The control problem is therefore expressed in the form of the computation of a set of camera velocities  $\mathbf{v}$  that ensure the transition from the current configuration  $\mathbf{s}$  to the desired  $\mathbf{s}^*$ :

$$\mathbf{v} = g(\mathbf{C} \times (\mathbf{s} - \mathbf{s}^*)_{1..n}) \quad (7)$$

where  $g()$  in our case is a simple proportional gain (but could be a more complex regulator),  $\mathbf{C}$  is a matrix that multiplies the "error" vector related to the  $n$  visual features.

The optimal choice for  $\mathbf{C}$  is to be the pseudo-inverse of the image Jacobian  $\mathbf{L}(\mathbf{s}, Z)^+$  which is normally computed by model, numerical approximation or estimation [7]. In our case we adopted the simplified choice to consider  $\mathbf{C}$  as a constant matrix equal to  $\mathbf{L}(\mathbf{s}^*, Z^*)^+$ , i.e. the pseudo-inverse of the interaction matrix computed for  $\mathbf{s} = \mathbf{s}^*$  and  $Z = Z^*$  where  $Z^*$  is an approximate value of  $Z$  at desired camera position. This is a convenient simplification that may have implications on the stability of the solution as described in [7], and the notable consequence that some visual features may get out of the camera field of view if the initial camera position is far away from the desired one. In our case we have found out that the low-pass filter realised by the typically slow dynamic response of a hovering AUV contributed positively towards the successful completion of the task. In addition to that, exploiting the axisymmetrical nature of the approaching maneuver, we have introduced a scheme to pre-select a suitable configuration  $\mathbf{s}^*$  from a precompiled list that best suit the initial orientation of the optical markers at first detection.

The typical performance obtained for the overall image servoing algorithm on the vehicle's 900 MHz dedicated embedded PC is of 12 frames per second. This has in turn proven to be sufficiently high to control our test ROV VORTEX in a number of simulated approach maneuvers, navigating the length of the test pool (3m) to docking configuration (see Fig. 7).

## V. CONCLUSIONS AND FUTURE WORK

We have developed a fully autonomous docking methodology for I-AUVs to perform an intervention task on ocean bottom seismographs. During the approach and the docking manoeuvres the motion controller of the vehicle is fed with processed information from sonar and image sensors, and the transition between the two phases is

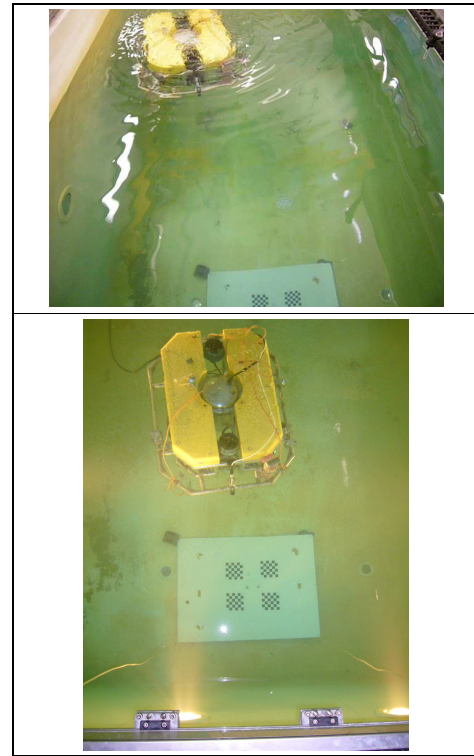


Fig. 7 – IFREMER's VORTEX during vision based test pool trials. The vehicle starts to dive (top) and reaches final configuration (bottom) after travelling the length of the pool.

performed automatically.

Having developed the core modules and built a 1:1 scale mock up of the docking structure, future work will focus on the continuation of extensive in-water experimentation both in test pool. and at sea. This phase will involve the use of our test vehicle VORTEX with the aim to improve and fine tune the various elements of the proposed method.

## REFERENCES

- [1] P. Oliveira, C. Silvestre, P. Aguiar, A. Pascoal, "Guidance and control of the SIRENE underwater vehicle: from system design to tests at sea", *Proceedings of the IEEE Int. Conf. OCEANS 1998*, 28(2):1043-1048, October 1998.
- [2] V. Rigaud, D. Semac, M. Drogou, J. Operbecke, C. Marfia, "From SIRENE to SWIMMER – Supervised Unmanned Vehicles: operational feedback from science to industry", *Proc. of the Int. Offshore Polar Engineering Conference, ISOPE'99*, Brest (France), June 1999.
- [3] M. Perrier, L. Brignone, "Optical stabilization for the ALIVE Intervention AUV", *Proc. of the 14<sup>th</sup> Int. Offshore Polar Engineering Conference, ISOPE'04*, Toulon (France), vol 2. pp. 230-250, May 2004.
- [4] unknown, "SEABEE – A mobile lander for autonomous monitoring and sampling", copyright 2007, internet page <http://www.uwth.unihamover.de/de/projekte/seabee/index.html>, accessed March 2007.
- [5] C.Harris, M.J. Stephens, "A combined corner and edge detector", *Proceedings of The Fourth Alvey Vision Conference*, Manchester, pp. 147-151. 1988.
- [6] E. Malis, F. Chaumette, S. Boudet, "2 1/2 D Visual servoing", *IEEE Transactions on Robotics and automation*, 15(2):238-250, April 1999.
- [7] F. Chaumette, E. Malis, "A possible solution to improve image-based and position based visual servoings", *Proc of the IEEE Int. Conf. on Robotics and Automation ICRA2000*, San Francisco, April 2000.